Wake and Potential Interference of Contra-Rotating Small-Sized Axial Fan at Design Flow Rate

Toru Shigemitsu[1]*, Hiroaki Fukuda[2], Junichiro Fukutomi[1]

ISROMAC 2016

International Symposium on Transport Phenomena and Dynamics of Rotating Machinery

Hawaii, Honolulu

April 10-15, 2016

Abstract

Small-sized axial fans are used as air coolers for electric equipment. There is a strong demand for high pressure and large flow rate of fans according to the increase of quantity of heat from electric devices. Therefore, high rotational speed design is conducted, although, it causes the deterioration of the efficiency and increase of noise. Then, the adoption of contra-rotating rotors for small-sized fans is proposed for the improvement of the performance. In the case of the contra-rotating rotors, the wake and potential interference between the front and rear rotors influence on the performance and stable operation. Therefore, it is necessary to clarify the internal flow between the front and rear rotors. In the present paper, pressure fluctuations around the rotor phase locked each front and rear rotor's rotation are shown and the influences of the wake and potential interference at a design flow rate are discussed by the unsteady numerical analysis results.

Keywords

Small-sized axial fan, Contra-rotating rotors, Wake, Potential interference

[1] *Institute of Technology and Science, Tokushima University,Tokushima, Japan*

[2] *Graduate School of Advanced Technology and Science, Tokushima University, Tokushima,Japan*

***Corresponding author**: t-shige@tokushima-u.ac.jp

INTRODUCTION

Because of spread of cloud computing, establishment of ubiquitous networking society and increase in rate of electric parts in machines, power consumption in data centers, IT devices and machines has been increasing significantly[1]. In the view of the issue of global warming and energy savings, there is a strong demand for the reduction of power consumption in above facilities and equipment. Electrical power used for the cooling of the IT devices for data centers is huge the same as that used for the IT devices itself in data centers. Small-sized axial fans are used as air coolers for electric equipment i.e. laptop, desk top computers and servers. There is a strong demand for high pressure and large flow rate of fans according to the increase of quantity of heat from electric devices. However, the increase of the pressure and flow rate by the increase of the fan diameter is restricted because of the limitation of the space. Therefore, high rotational speed design is conducted, although, it causes the deterioration of the efficiency and increase of the noise. On the other hand, lower rotational speed design[2] and advantages on the performance of the contra-rotating fans and pumps were verified by experimental results[3],[4]. Then, the adoption of the contra-rotating rotors for the small-sized axial fans was proposed for the improvement of the performance. In the case of contra-rotating rotors, the axial space becomes larger than conventional small-sized axial fans. However, it is adequate choice to apply the contra-rotating rotors for small-sized fan because the axial space can be ensured in electrical devices as compared to that of the radial space.

In the case of the contra-rotating rotors, it is necessary to design the rear rotor considering the unsteady circumferential velocity distributions at the outlet of the front rotor[5]. Further the fan noise becomes larger than the conventional rotor stator type fan because of the interaction between the front and rear rotors. Then, the passive noise reductions with the peforated blade was propsed for the contra-rotating fan[6]. It is important to clarify the influence of the wake from the front rotor to the rear rotor and the potential interaction between the front and rear rotors to increase the performance and to reduce the fan noise[7]. The blade row distance between front and rear rotors is a key parameter to consider the wake and potential interaction for the contra-rotating fan. The influence of the blade row distance between the front and rear rotors and pressure fluctuation on the casing wall were investigated for the counter rotating fan with fan diameter D=375mm[4],[8]. On the other hand, the conventional design method and the theory for the turbo machinery should be modified for small-sized axial fans because small-sized axial fans applied to electrical devices belong to extremely small size field in the turbo machinery[9]. Therefore, there is the strong demand to establish the design method for small-sized axial fans based on the internal flow between the front and rear rotors.

In the present paper, the performance curves of the contra-rotating small-sized axial fan with 100mm diameter are compared with the unsteady numerical analysis results to verify the validity of the unsteady numerical analysis results. After that, pressure fluctuations around the rotor phase locked each front and rear rotor's rotation are shown and the influences of the wake and the potential interference at the design flow rate are discussed by the unsteady numerical analysis results.

1. EXPERIMENTAL APPARATUS AND METHOD

The geometry of the rotor and the primary dimensions of the contra-rotating small-sized axial fan (RRtype) are shown in Fig.1 and Table 1, respectively. The hub tip ratio was D_h/D_t=45[mm]/98[mm], tip clearance was c=1[mm] and the design flow rate was Q_d=0.016[m^3/s]. Fan static pressure at the design point was P_{dRR}=14.7[Pa] for RRtype with the same fan static pressure of each front and rear rotor. The rotational speed of front and rear rotors of RRtype was N_f=N_r=1780[min^{-1}]. This fan was designed with the free vortex design. In this research, an aerofoil blade was used because there was a report that implied an advantage of the airfoil blade for the small-sized axial fan[10], however a circular-arc blade was generally used for small-sized axial fans. Figure 2 shows the schematic diagram of the experimental apparatus for RRtype. The experimental apparatus was designed based on the Japanese Industrial Standard and the air blown in the test section passed the rotor, chamber, measurement duct and booster fan and blew out in the ambient atmosphere. The fan static pressure (P_s) was measured by the pressure difference between static holes downstream of the rotor installed at the chamber and ambient air. The fan static pressure of each front and rear rotor was also measured to investigate pressure curves of each front and rear rotor in wide flow rates range. Further, the rotational speed was controlled by the servo motor and the flow rates were measured by the orifice meter set at the measurement duct. The pressure curves of RRtype from the cutoff flow rate to the large flow rate were investigated in the experiment with the constant rotational speed N_f=N_r=1780[min^{-1}]. In this research, the performance test was conducted with two different blade row distances L=10[mm] (non-dimensional axial distance divided by front rotor tip chord length L/l_{FR}=0.42), 30[mm](L/l_{FR}=1.27). L was defined as the axial distance from the trailing edge of the front rotor to the leading edge of the rear rotor at the hub.

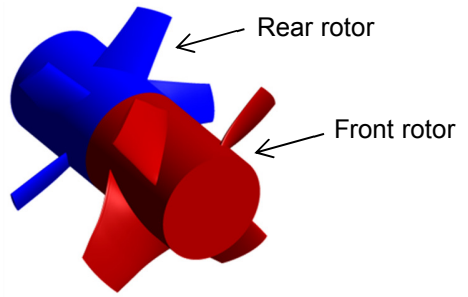

Figure. 1 Contra-rotating small-sized axial fan (RRtype)

Table. 1 Primary dimensions of RRtype

		Hub	Mid	Tip
	Diameter[mm]	45	72	98
Front Rotor	Blade Number	4		
	Blade Profile	NACA 4409		
	Solidity	1.196	0.496	0.29
	Stagger Angle	44.7°	61.1°	68.2°
Rear Rotor	Blade Number	5		
	Blade Profile	NACA 4412		
	Solidity	0.91	0.447	0.288
	Stagger Angle	56.7°	64.5°	69.6°

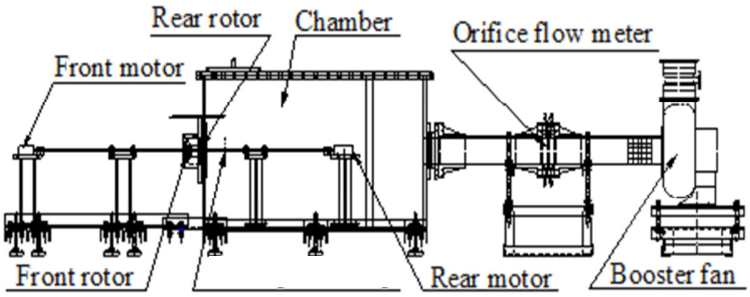

Figure. 2 Experimental apparatus

2. NUMERICAL ANALYSIS CONDITIONS

The commercial software ANSYS-CFX 14.5 was used to investigate the flow condition and potential interference between the front and rear rotors of the contra-rotating small-sized axial fan which couldn't be measured by the experiment. In the numerical analysis, the numerical model which was almost the same with the experimental apparatus was used and three dimensional unsteady numerical analysis was conducted. The numerical analysis grids used for the numerical analysis are shown in Fig.3. To simplify the numerical analysis, the servo motors and the shafts of the servo motors are removed in the numerical analysis model. The numerical domains comprised the inlet, rotor, chamber and outlet duct regions. The numerical grid elements were 617,090 for the inlet region, 1,479,336 for the chamber region and 237,628 for the outlet duct region. The numerical grid elements for the rotor region were 5,542,038 (L=10[mm]) or 6,038,826 (L=30[mm]) for RRtype. The tip clearance kept 1mm as the same with the experimental apparatus in the numerical analysis and the number of elements from the blade tip to the casing was 7. At the inlet boundary, the uniform velocity was given and the constant pressure was given at the outlet boundary condition. The coupling between the front and rear rotors was conducted by the sliding mesh (Transient Rotor Stator Model). The Near-Wall Treatment "Automatic" and SST (Shear Stress Transport) turbulence model were used. The unsteady numerical analysis was

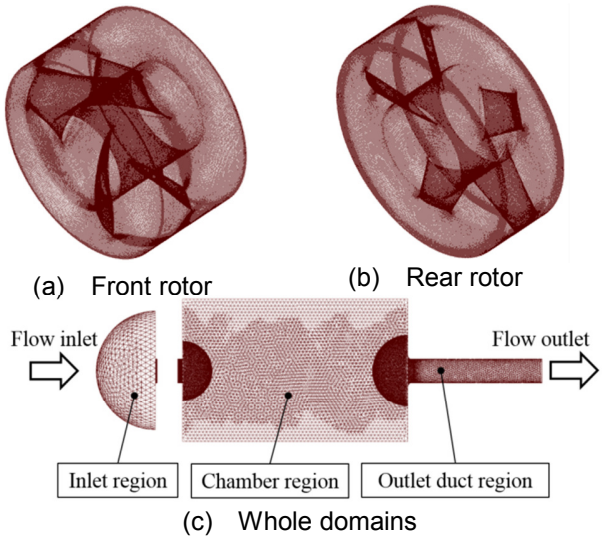

Figure. 3 Numerical analysis grids

conducted at six flow rates (0.01Qd, 0.1Q_d, 0.6Q_d, 0.9Q_d, 1.0Q_d and 1.2Q_d). The time step number per one rotor rotation was 180 and the time step was Δt=1.8727×10^{-4} [s] (corresponding 2° of the rotor rotation). The data of one rotor rotation were obtained after 6 rotor rotations in unsteady numerical analysis. The convergence criteria at each time step were set as the residual less than 1.0×10^{-4}.

3. EXPERIMENTAL AND NUMERICAL ANALYSIS RESULTS

3.1 Performance curve of RRtype

The fan static pressure curves of RRtype at each blade row distance (L=10, 30[mm]) are shown in Fig.4. In Fig.4, the fan static pressure obtained by both experiment and numerical analysis are shown. In the unsteady numerical analysis, the fan static pressure was obtained at the same point in the experiment and 180 static pressure data of one rotor rotation were averaged. The vertical axis and horizontal axis in Fig.4 show the fan static pressure P_s and flow rate Q. It was found from Fig.4 that fan static pressure of RRtype linearly increased as the flow rate decreased, and the pressure curve of RRtype showed the stable negative curve. The fan static pressure curves of the front rotor and rear rotor are shown in Fig.5. The fan static pressure of the front rotor also showed the same tendency of RRtype, but the fan static pressure of the rear rotor represented a different tendency from the fan static pressure of RRtype in the partial flow rates. And the slight positive slope of the pressure curve was confirmed in the low flow rates for the rear rotor. It was clarified from the previous research[11] that the fan static pressure kept almost constant by the blade row distance L=30[mm] (L/l_{FR}=1.27). It was confirmed from Fig.4 that the difference of the fan static pressure between L=10[mm] and L=30[mm] was P_s=0.02 (Exp.) at the design flow rate Q_d=0.016[m^3/s]. The influence of the blade row distance in the range of L=10-30[mm] on the fan static pressure was small. The numerical analysis results could predict the experimental results accurately and capture the tendency of the performance curves of the experimental results. It was difficult to measure the efficiency of this small fan. Therefore, the efficiency of the test fan was investigated by the numerical analysis results. The static pressure efficiency of RRtype for L=10[mm] and 30[mm] is shown in Fig.6. The maximum static pressure efficiency was η=58.0% for L=10[mm] and η=57.0% for L=30[mm] and the difference of the efficiency for L=10[mm] and 30[mm] were small in wide flow rate range. The static pressure efficiency of each front and rear rotors are shown in Fig.7. The static pressure efficiency of the rear rotor was larger than that of the front rotor especially around the design flow rate. The static pressure efficiency of the front rotor for L=30[mm] was larger than that for L=10[mm] at the design flow rate and vice versa in the case of the rear rotor. It is important to clarify the wake and potential interference for the stable operation of the contra-rotating small sized fan, therefore, the interferences at the design flow rate were investigated by the unsteady numerical analysis.

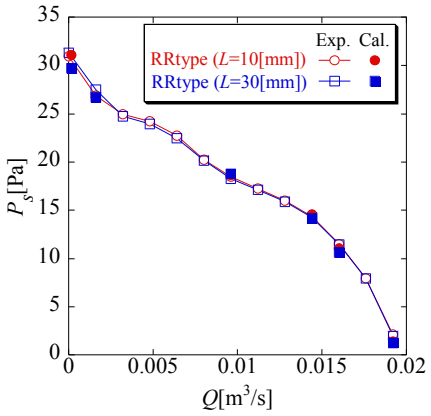

Figure. 4 Fan static pressure of RRtype

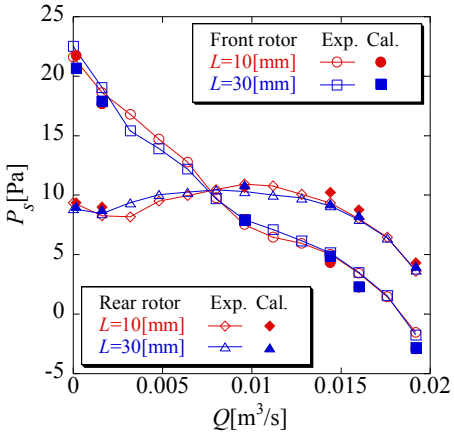

Figure. 5 Fan static pressure of each front and rear rotor

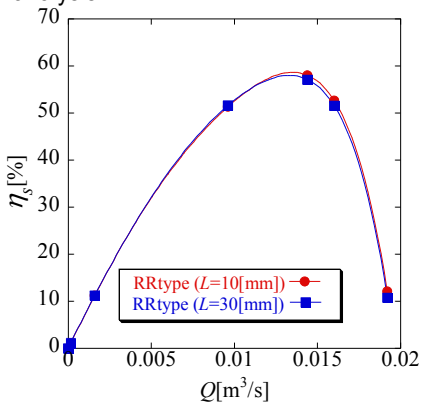

Figure. 6 Fan static pressure efficiency of RRtype

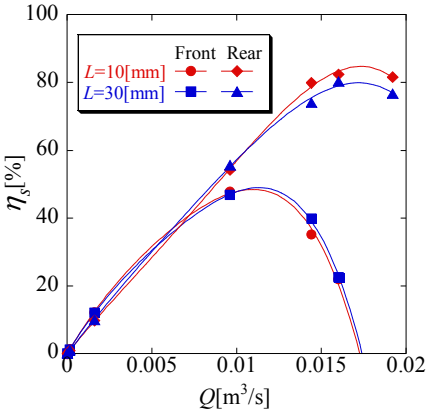

Figure. 7 Fan static pressure efficiency of each front and rear rotor

3.2 Wake and potential interference between front and rear rotors (*L*=10, 30[mm])

In this section, the pressure fluctuations around the rotor phase locked each front and rear rotor's rotations are shown and the influences of the wake and potential interference are discussed by the unsteady numerical analysis results. The sampling points for pressure fluctuations and definition of the relative position of the front and rear rotors are shown in Fig.8. The respective data for the front rotor were obtained at the middle position of the pressure surface (PS) of the blade and 0.1[mm] downstream from the trailing edge (TE) of the front rotor. And the data for the rear rotor were obtained at the middle position of the suction surface (SS) of the blade and 0.1mm upstream from the leading edge (LE) of the rear rotor. The rotational angles of the front and rear rotors are shown as θ_f, θ_r respectively. The rotational angles were defined as the angles of the 25% chord length position of each front and rear rotor from the arbitrary meridional plane. The relative angle of the front and rear rotors θ_{fr} are defined as $\theta_{fr}=\theta_f+\theta_r$, the initial relative angle is θ_{fr}=0[deg.] ($\theta_f=\theta_r$=0[deg.]). The rotational direction of the angle θ_f, θ_r were the same with the rotational direction of the front and rear rotors respectively. The pressure fluctuations at the middle position of the PS and the TE of the front rotor at the design flow rate Q_d=0.016[m^3/s] obtained by the numerical analysis are shown in Figs.9 and 10 respectively. The vertical axis is the fluctuation of the static pressure ΔP_s from the averaged value and the horizontal axis is the relative angle of the front and rear rotors θ_{fr}. Further, r/r_c shows non-dimensional radius divided by the radius at the casing; r/r_c=0.45 and r/r_c=1.0 correspond the hub and casing. Because the pressure in Figs.9 and 10 were phase locked the front rotor, the potential interference from the rear rotor became clear if the unsteady pressure fluctuations from the front rotor were small. The periodic fluctuations with five peaks corresponding to the rear rotor blade number Z_R=5 were generated for the blade row distance *L*=10mm and *L*=30mm in Figs.9 and 10. The pressure fluctuations ΔP_s at the middle position of the PS of the front rotor for *L*=10mm and *L*=30mm were within ±0.75Pa (fan static pressure P_s=11.47Pa at Q_d for *L*=10mm) and ±0.25Pa (fan static pressure P_s=11.45Pa at Q_d for *L*=30[mm]) respectively. On the other hand, the pressure fluctuations ΔP_s at the TE of the front rotor for *L*=10mm and *L*=30[mm] were within ±1.2[Pa] and ±0.3[Pa] respectively. The pressure fluctuation became small as the distance from the rear rotor became large and the potential interference of the rear rotor could be suppressed with the increase of the blade row distance from *L*=10[mm] to *L*=30[mm].

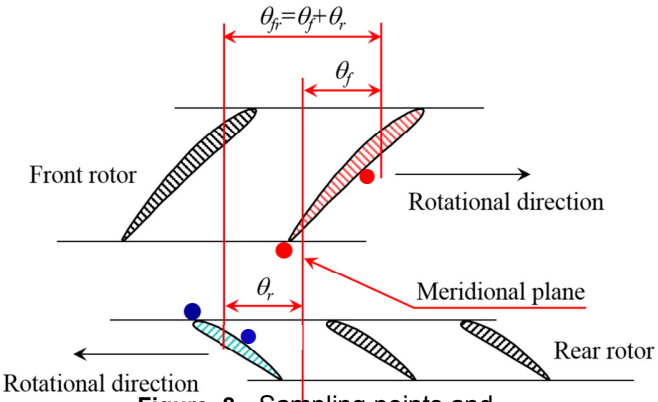

Figure. 8 Sampling points and relative position of front and rear rotors

The pressure fluctuations at the LE and the middle position of the SS of the rear rotor obtained by the numerical analysis are shown in Figs.11 and 12 respectively. The flow rate, vertical axis and horizontal axis are the same in Figs.9 and 10. Because the pressure in Figs.11 and 12 were phase locked the rear rotor, the wake and potential interference from the front rotor became clear if the unsteady pressure fluctuations from the rear rotor were small. The periodic pressure fluctuations with four peaks corresponding to the front rotor blade number Z_F=4 were generated for the blade row distance *L*=10mm and *L*=30mm in Figs.11 and 12. The pressure fluctuations ΔP_s at the LE of the rear rotor were larger than that at the TE of the front rotor. The pressure fluctuations ΔP_s at the LE and middle position of the SS of the rear rotor near the shroud at r/r_c=0.98 were significantly large compared to the other radial positions. These large pressure fluctuations near the shroud would be related to the flow condition at the rear rotor inlet. When the pressure fluctuations ΔP_s of the front and rear rotors were compared,

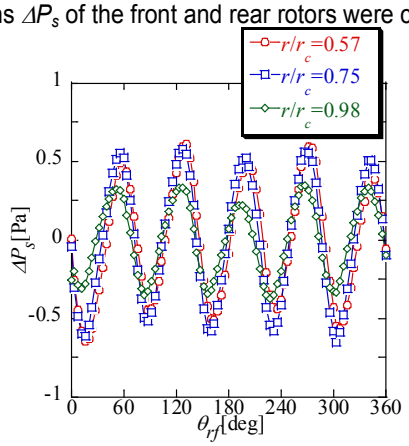

(a) *L*=10mm

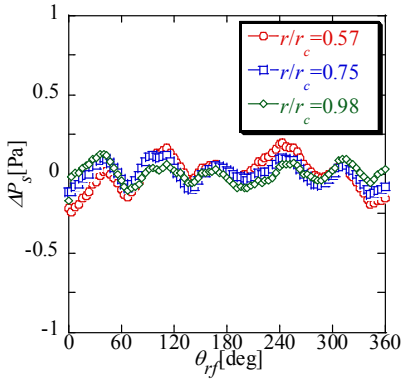

(b) *L*=30mm

Figure. 9 Pressure fluctuations at middle position of PS of front rotor

the pressure fluctuations ΔP_s of the rear rotor larger than that of front rotor as shown in Figs.9-12. The variation of the blade loading of the rear rotor with the rotor rotation caused by the pressure fluctuations in Figs.11 and 12 would be larger than that of the front rotor. Therefore, it is important to consider the influence of the wake and potential interferences especially on the rear rotor for the stable operation of the contra-rotating small sized fan. On the other hand, the wake and potential interference from the front rotor could be suppressed with the increase of the blade row distance from L=10mm to L=30[mm] as shown in Figs.11 and 12.

The pressure fluctuations of the rear rotor were large. Then, the attack angle variations with the rotor rotation at the design flow rate Q_d were obtained by the numerical analysis. Figure 13 shows the attack angle variations of the rear rotor with the rotors rotation. The vertical axis is attack angle and the horizontal axis is the relative angle of the front and rear rotors θ_{fr}. The attack angle variation of the rear rotor for L=10[mm] were larger than that for L=30[mm]. It was considered that the wake from the front rotor would influence on the attack angle of the rear rotor. The variation of the attack angle might induce the pressure fluctuations in Fig.11. The pressure fluctuations and attack angle variation were suppressed for the blade row distance L=30[mm]. Therefore, the blade row distance L=30mm would be

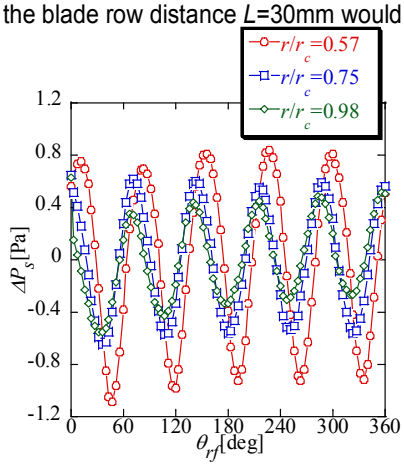

(a) L=10mm

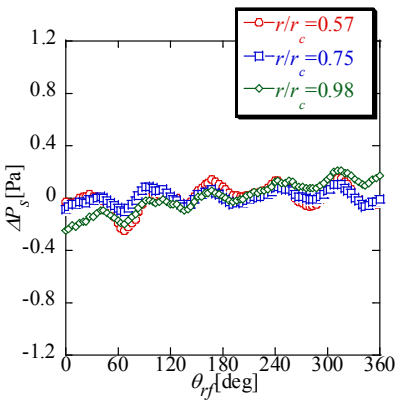

(b) L=30mm

Figure. 10 Pressure fluctuations at TE of front rotor

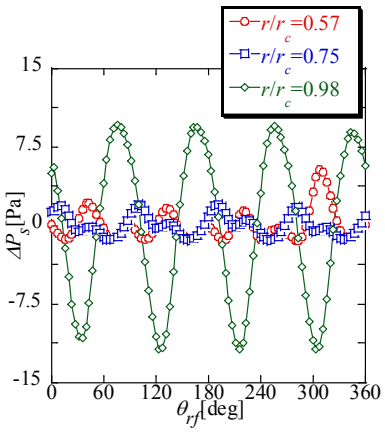

(a) L=10mm

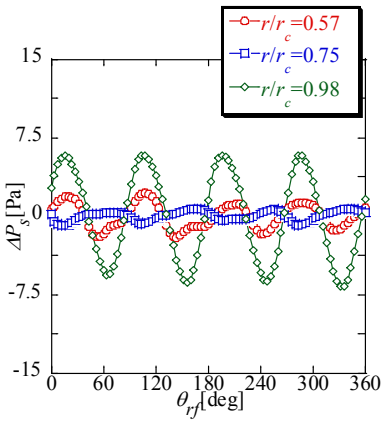

(b) L=30mm

Figure. 11 Pressure fluctuations at LE of rear rotor

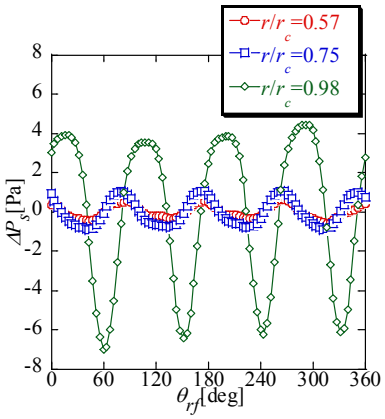

(a) L=10mm

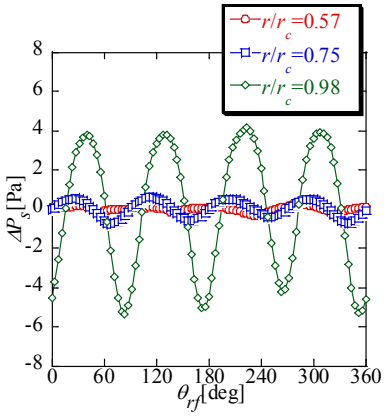

(b) L=30mm

Figure. 12 Pressure fluctuations at middle position of SS of rear rotor

appropriate blade row distance because the performance decrease with the increase of the blade row distance was small by L=30mm and the wake and potential interference could be suppressed effectively for L=30mm.

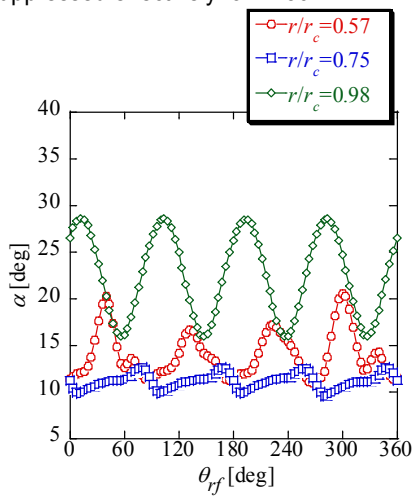

(a) L=10mm

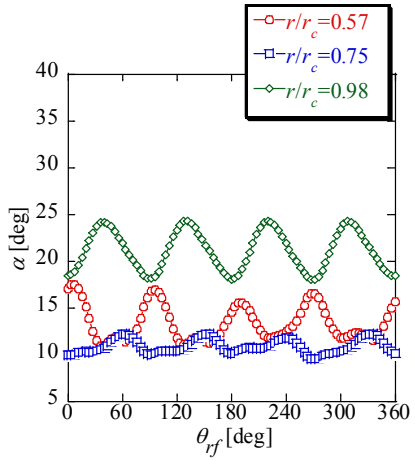

(b) L=30mm

Figure. 13 Attack angle variations of rear rotor with rotation

ACKNOWLEDGMENTS

The authors wish to show our special thanks to the supports by the Komiya research aid, the project research aid from The University of Tokushima and Japan Science and Technology Agency.

REFERENCES

[1] Hata, T and Nakamoto, S., 2010, "Energy Saving Service for Data Centers", *Journal the Japan Society for Precision Engineering*, Vol.76, No.3, pp.272-275.

[2] Furukawa, A., Shigemitsu, T and Watanabe, S., "Performance Test and Flow Measurement of Contra-Rotating Axial Flow Pump," *Journal of Thermal Science*, Vol. 16, No. 1, pp. 7 – 13, 2007.

[3] Furukawa, A., Cao, Y., Okuma, K and Watanabe, S., "Experimental Study of Pump Characteristics of Contra-Rotating Axial Flow Pump," *Proc. 2nd Int. Symposium on Fluid Machinery and Fluid Engineering*, Beijing, 67-657, pp. 245 – 252, 2000.

[4] Nouri, H., Ravelet, F., Bakir, F., Sarraf, C and Rey, R., "Design and Experimental Validation of a Ducted Counter-Rotating Axial-Flow Fans System," *Journal of Fluids Engineering*, Vol.134, No.10, 104504, doi:10.1115/1.4007591, 2012.

[5] Shigemitsu, T., Furukawa, A., Okuma, K and Watanabe, S., "Experimental Study on Rear Rotor Design in Contra-Rotating Axial Flow Pump," *Proceedings of 5th JSME/ KSME Fluids Engineering Conference*., Nagoya, pp. 1453 – 1548, 2002.

[6] Wang, C and Huang, L., "Passive Noise Reduction for a Contrarotating Fan," *Journal of Turbomachinery*, Vol.137, No.3, 031007, doi:10.1115/1.4028357, 2014.

[7] Sanders, A, J., Papalia, J and Fleeter, S., "Multi-Blade Row Interactions in a Transonic Axial Compressor: Part I - Stator Particle Image Velocimetry (PIV) Investigation," *Journal of Turbomachinery*, Vol. 124, pp. 10 – 18, 2002.

[8] Nouri, H., Danlos, A., Ravelet, F., Bakir, F and Sarraf, C., "Experimental Study of the Instationary Flow Between Two Ducted Counter-Rotating Rotors," *Journal of Engineering*

4. CONCLUDING REMARKS

The performance test of the contra-rotating small-sized axial fan was conducted under the condition of different blade row distance. Then, the wake and potential interference between the front and rear rotors were investigated at the design flow rate Q=0.016[m^3/s] with the unsteady numerical analysis. As a result, following concluding remarks could be obtained.

1. The difference of the fan static pressure between L=10[mm] and L=30[mm] was P_s=0.02 (Exp.) at the design flow rate Q_d=0.016[m^3/s]. The maximum static pressure efficiency was η=58.0% for L=10[mm] and η=57.0% for L=30[mm]. The influences of the blade row distance in the range of L=10-30[mm] on the fan static pressure and static pressure efficiency were small.

2. The periodic pressure fluctuations corresponding to the blade number of each front and rear rotor were confirmed at the LE of the rear rotor and TE of the front rotor respectively. The potential interference from the rear rotor could be suppressed with the increase of the blade row distance from L=10[mm] to L=30[mm]. The wake and potential interference from the front rotor could be suppressed also with the increase of the blade row distance from L=10[mm] to L=30[mm].

3. The attack angle variation of the rear rotor for L=10[mm] were larger than that for L=30[mm]. It was considered that the wake from the front rotor would influence on the attack angle of the rear rotor. The blade row distance L=30[mm] would be appropriate blade row distance because the performance decrease with the increase of the blade row distance was small by L=30[mm] and the wake and potential interference could be suppressed effectively for L=30[mm].

for Gas Turbines and Power, Vol.135, No.2, 022601, doi:10.1115/1.4007756, 2013.

[9] Shigemitsu, T., Fukutomi, J and Okabe, Y., "Performance and Flow Condition of Small-Sized Axial Fan and Adoption of Contra-Rotating Rotors," *Journal of Thermal Science*, Vol. 19, No. 1, pp. 1 – 6, 2010.

[10] Ito, T., Minorikawa, G., Nagamatsu, A and Suzuki, S., "Experimental Research for Performance and Noise of Small Axial Flow Fan (Influence of Parameter of Blade)," *Transactions of the JSME (in Japanese)*, Vol. 72, No. 715, pp. 670 – 667, 2006.

[11] Shigemitsu, T., Fukutomi, J and Shimizu H., "Influence of Blade Row Distance on Performance and Flow Condition of Contra-Rotating Small-Sized Axial Fan", *International Journal of Fluid Machinery and Systems*, Vol.5, No.4, pp.161-167, 2012.